

Theoretical assessment of the behavior of cable bracing system with central steel cylinder

Advances in Structural Engineering
2016, Vol. 19(3) 463–472
© The Author(s) 2016
Reprints and permissions:
sagepub.co.uk/journalsPermissions.nav
DOI: 10.1177/1369433216630052
ase.sagepub.com



Nader Fanaie¹, Saeid Aghajani² and Ebrahim Afsar Dizaj³

Abstract

Different kinds of bracing systems are used as the basic methods for providing lateral stiffness and strength in building frames. In recent years, tension-only bracing systems have been suggested by researchers. Steel cable has been recognized as a flexible member which can tolerate tensional forces only. Using the tension-only members as bracing for structures has triggered the concept of applying cables as the lateral braces of structures. Despite the high stiffness and tensional strength of steel cables, they cannot be considered as proper devices in cross bracing due to their low ductility. One of the modern bracing systems is using cables along with a cylinder through which a pair of cables passes from their crossing point. Such bracing systems can be used in strengthening of moment-resisting frames. This research presents the equations that are related to the behavior of cable steel cylinder bracing. Also, the effects of cylinder dimensions and prestressing of cables on the behavior of the mentioned bracing were assessed. In such bracing with steel cylinder, both cables are under tension; therefore, the loosening of cables and their ability to cause impulses will be removed. Moreover, the cables reach their final strengths at higher frame lateral displacements. It is recommended to select the dimensions of the cylinder in such a way that the cables also reach their yielding limit in the damage limit displacement of the frame.

Keywords

cable bracing, lateral stiffness, prestressing force, steel cylinder

Introduction

Efficiency and performance of structures have direct relations with the available material and construction technology. Overtime, considerable progress has been achieved in recognizing and presenting new materials, methods, construction devices, and servicing.

Cables, one of the important structural components, are defined as flexible tensile members with slight flexural stiffness. Cables with high ratios of strength to weight have different applications in structures (Jeong-In and Sung Pil, 2000). They are often used in bridges and large roofs (Ben Mekki and Auricchio, 2011; Kang et al., 2014; Osamu et al., 1999; Straupe and Paeglitis, 2013; Wu et al., 2006) but not ordinarily in buildings. In recent years, researchers have been motivated to study the application of cables in buildings in different ways concerning their advantages. Some of researchers have focused on using cables in tall buildings for controlling frame lateral displacement (Saleem and Saleem, 2010). Some others have been concerned with applying the cables instead of shear reinforcement in reinforced concrete beams (Keun-Hyeok et al., 2011). Several researchers have scrutinized the use of

cables for preventing progressive damages of structures (Hadi and Saeed Alrudaini, 2012; Tan and Astaneh-Asl, 2003) and bridges (Cai et al., 2012). In recent years, different kinds of cable bracings have been presented by researchers (Chuang et al., 2004; Kurata et al., 2012; Razavi and Sheidaii, 2012; Zahrai and Hamidia, 2009). Some of the advantages of using wire-ropes as bracings are as follows: flexibility, high capacity in supporting the tensional forces, simple design, fast and easy construction and installation, no heavy devices for installation, and creating the least noises during installation (Kurata et al., 2012).

¹Faculty of Civil Engineering, K. N. Toosi University of Technology, Tehran, Iran

²Structural Engineering, Faculty of Civil Engineering, K. N. Toosi University of Technology, Tehran, Iran

³Structural Engineering, Faculty of Engineering, University of Guilan, Rasht, Iran

Corresponding author:

Ebrahim Afsar Dizaj, Structural Engineering, Faculty of Engineering, University of Guilan, Rasht, Iran.
Email: ebrahim_afsar@live.com

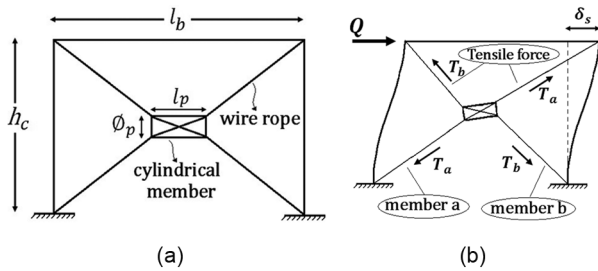


Figure 1. Cable bracing system with central cylinder: (a) dimensions and (b) deformation at δ_s .

Cable bracing system with central cylinder is one of the modern bracing systems in which a pair of cables passes through the cylinder in their interaction point. In such systems, the cables and cylinder are used in such a way that the cables reach their final strengths at higher frame lateral displacements and therefore cover their ductility defects as shown in Figure 1 (Hou and Tagawa, 2009). Hou and Tagawa (2009) used this bracing system for seismic retrofit of steel moment frames and concluded that this retrofitting method can increase the lateral story strength without reducing the moment frame ductility; moreover, it restrains the story drift to within the specified range. Figure 2 shows the test setup of their research.

The behavior of this bracing system depends on the dimensions of the cylinder as well as the axial rigidity and prestressing of the cables. Theoretical behavior of this bracing system has been studied in the case of using soft cylinder (Fanaie et al., 2012). In this

research, the behavior of the mentioned system is assessed in the case of using a stiff cylinder such as a steel cylinder. This study focuses on the effect of cylinder dimensions and prestressing of cables.

Governing equations

A cylinder with high stiffness and very low elastic deformation like a steel cylinder can be considered rigid for simplicity of calculations. In such states under lateral static displacement of the frame (δ) toward the right, the center of the horizontal cylinder moves as $\delta/2$ and rotates as θ in the counterclockwise direction. The displacement of the cylinder center in the vertical direction is 0.

In this section, the relation between the lateral displacement of the frame and rotation of the cylinder is presented using the equilibrium equation of the cylinder. Then, the equations needed for plotting the curves of $P-\delta$ and $\varepsilon-\delta$ are obtained. Figure 3 is used for achieving the equations governing the behavior of rigid cylinder-cable bracing. In this figure which represents a simple frame, the coordinate axes are identified as well.

It is assumed that the cylinder is located at the center of frame. Considering this assumption, the slopes of AE and GC are equal and the slopes of BF and HD are equal as well. According to Figure 3, if the length of the beam = l_b , height of column = h_c , length of cylinder = u , and the inner diameter of cylinder-cable = v , then the lateral displacement of the frame (δ) is obtained as follows

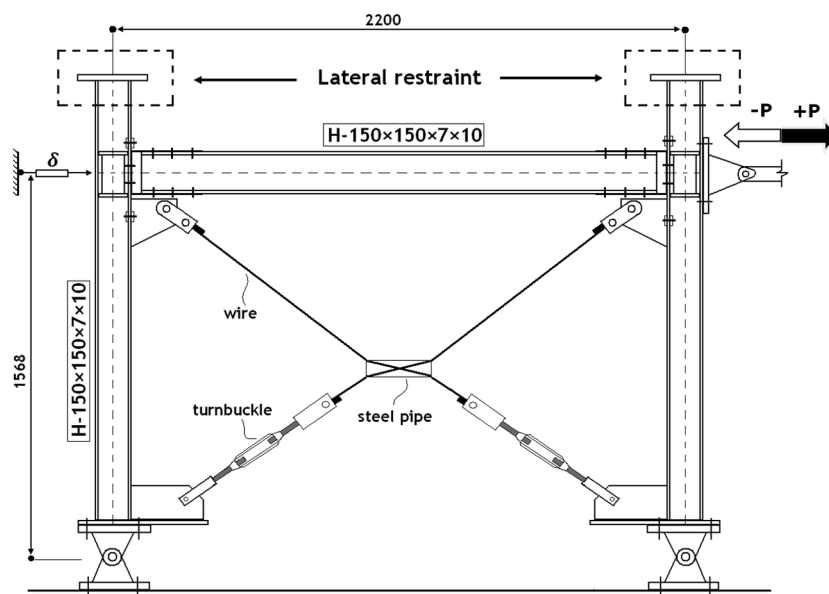


Figure 2. Test setup (Hou and Tagawa, 2009).

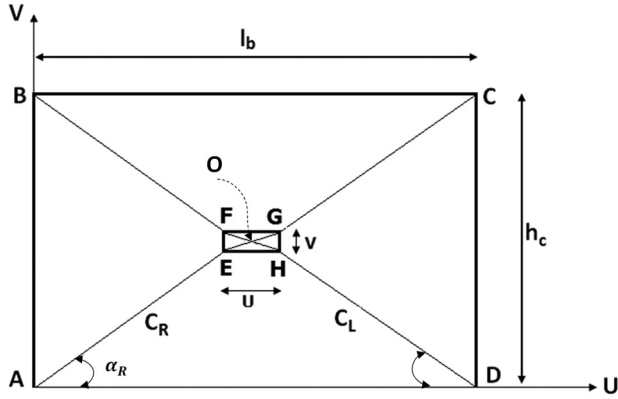


Figure 3. The frame with rigid cylinder-cable bracing.

$$A : \begin{bmatrix} 0 \\ 0 \end{bmatrix}$$

$$B : \begin{bmatrix} \delta \\ h_c \end{bmatrix}$$

$$C : \begin{bmatrix} l_b + \delta \\ h_c \end{bmatrix}$$

$$D : \begin{bmatrix} l_b \\ 0 \end{bmatrix}$$

$$E : \frac{1}{2} \begin{bmatrix} (l_b + \delta) - u \cos \theta + v \sin \theta \\ h_c - u \sin \theta - v \cos \theta \end{bmatrix}$$

$$F : \frac{1}{2} \begin{bmatrix} (l_b + \delta) - u \cos \theta - v \sin \theta \\ h_c - u \sin \theta + v \cos \theta \end{bmatrix}$$

$$G : \frac{1}{2} \begin{bmatrix} (l_b + \delta) + u \cos \theta - v \sin \theta \\ h_c + u \sin \theta + v \cos \theta \end{bmatrix}$$

$$H : \frac{1}{2} \begin{bmatrix} (l_b + \delta) + u \cos \theta + v \sin \theta \\ h_c + u \sin \theta - v \cos \theta \end{bmatrix}$$

$$O : \frac{1}{2} \begin{bmatrix} l_b + \delta \\ h_c \end{bmatrix}$$

where θ is the rotation of the cylinder. The equilibrium equation of cylinder should be used for obtaining the relation between cylinder rotation and lateral displacement of the frame. The cylinder should rotate in such a way that the applied moment from the cables to the cylinder becomes equal to 0 (Figure 4).

The equilibrium equation of a cylinder is as follows

$$\sum M = 0 \rightarrow F_R \times \frac{|\overrightarrow{AE} \times \overrightarrow{EG}|}{|\overrightarrow{AE}|} = F_L \times \frac{|\overrightarrow{DH} \times \overrightarrow{FH}|}{|\overrightarrow{DH}|} \quad (1)$$

where F_R and F_L are the forces of the right and left cables, respectively; it is calculated as follows

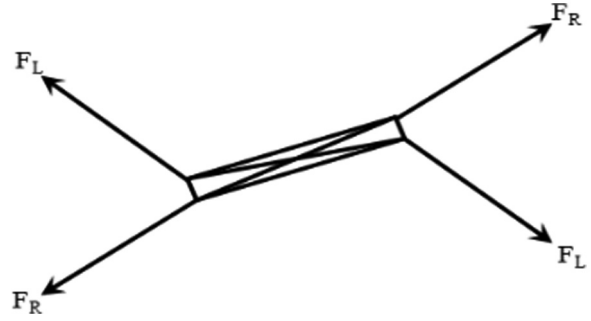


Figure 4. Free body diagram of rigid cylinder.

$$F_R = \frac{AE}{L_{AE} + L_{EO}} \times \Delta_{AE} \quad (2)$$

$$F_L = \frac{AE}{L_{DH} + L_{HO}} \times \Delta_{DH} \quad (3)$$

where AE is the axial rigidity of each cables, and Δ_{AE} and Δ_{DH} are the elongation of cables AE and DH , respectively. Considering the equal lengths and axial rigidity values for both right and left cables, the equilibrium equation of the cylinder is expressed as follows

$$\sum M = 0 \rightarrow \Delta_{AE} \times \frac{|\overrightarrow{AE} \times \overrightarrow{EG}|}{|\overrightarrow{AE}|} = \Delta_{DH} \times \frac{|\overrightarrow{DH} \times \overrightarrow{FH}|}{|\overrightarrow{DH}|} \quad (4)$$

The above equation has been expressed based on the initial lengths of cables, elongation of cables, and cross product of directions of cables in and out of the cylinder. They are the functions of lateral displacement of the frame and dimensions and also rotation of cylinder, written as follows

$$\overrightarrow{AE} = \frac{1}{2} \begin{bmatrix} (l_b + \delta) - u \cos \theta + v \sin \theta \\ h_c - u \sin \theta - v \cos \theta \end{bmatrix} \quad (5)$$

$$\overrightarrow{EG} = \begin{bmatrix} u \cos \theta - v \sin \theta \\ u \sin \theta + v \cos \theta \end{bmatrix} \quad (6)$$

$$\overrightarrow{FH} = \begin{bmatrix} u \cos \theta + v \sin \theta \\ u \sin \theta - v \cos \theta \end{bmatrix} \quad (7)$$

$$\overrightarrow{DH} = \frac{1}{2} \begin{bmatrix} (l_b - \delta) - u \cos \theta - v \sin \theta \\ -h_c - u \sin \theta + v \cos \theta \end{bmatrix} \quad (8)$$

$$|\overrightarrow{AE} \times \overrightarrow{EG}| = \frac{1}{2} |(l_b + \delta)(u \sin \theta + v \cos \theta) - h_c(u \cos \theta - v \sin \theta)| \quad (9)$$

$$\begin{aligned} |\overrightarrow{DH} \times \overrightarrow{FH}| &= \\ \frac{1}{2} |(l_b - \delta)(u \sin \theta - v \cos \theta) + h_c(u \cos \theta + v \sin \theta)| & \end{aligned} \quad (10)$$

$$\begin{aligned} |\overrightarrow{AE}| &= \\ \frac{1}{2} \sqrt{((l_b + \delta) - u \cos \theta + v \sin \theta)^2 + (h_c - u \sin \theta - v \cos \theta)^2} & \end{aligned} \quad (11)$$

$$\begin{aligned} |\overrightarrow{DH}| &= \\ \frac{1}{2} \sqrt{((l_b - \delta) - u \cos \theta - v \sin \theta)^2 + (-h_c - u \sin \theta + v \cos \theta)^2} & \end{aligned} \quad (12)$$

$$\begin{aligned} \Delta_{AE} &= \\ \frac{1}{2} \sqrt{((l_b + \delta) - u \cos \theta + v \sin \theta)^2 + (h_c - u \sin \theta - v \cos \theta)^2} & \\ - \frac{1}{2} \sqrt{(l_b - u)^2 + (h_c - v)^2} & \end{aligned} \quad (13)$$

$$\begin{aligned} & \left[1 - \frac{\sqrt{(l_b - u)^2 + (h_c - v)^2}}{\sqrt{((l_b + \delta) - u \cos \theta + v \sin \theta)^2 + (h_c - u \sin \theta - v \cos \theta)^2}} \right] \\ & \times |(l_b + \delta)(u \sin \theta + v \cos \theta) - h_c(u \cos \theta - v \sin \theta)| \\ & = \left[1 - \frac{\sqrt{(l_b - u)^2 + (h_c - v)^2}}{\sqrt{((-l_b + \delta) + u \cos \theta + v \sin \theta)^2 + (h_c + u \sin \theta - v \cos \theta)^2}} \right] \\ & \times |(-l_b + \delta)(-u \sin \theta + v \cos \theta) + h_c(u \cos \theta + v \sin \theta)| \end{aligned} \quad (15)$$

The angles of the external parts of the cables are expressed as follows.

$$\begin{aligned} \cos \alpha_R = \cos \alpha_{\overrightarrow{AE}} &= \\ \frac{(l_b + \delta) - u \cos \theta + v \sin \theta}{\sqrt{((l_b + \delta) - u \cos \theta + v \sin \theta)^2 + (h_c - u \sin \theta - v \cos \theta)^2}} & \end{aligned} \quad (16)$$

$$\begin{aligned} -\cos \alpha_L = \cos \alpha_{\overrightarrow{DH}} &= \\ \frac{(-l_b + \delta) + u \cos \theta + v \sin \theta}{\sqrt{((-l_b + \delta) + u \cos \theta + v \sin \theta)^2 + (h_c + u \sin \theta - v \cos \theta)^2}} & \end{aligned} \quad (17)$$

α_R and α_L are shown in Figure 3.

Equation (18) is used for plotting P - δ curve.

$$\begin{aligned} \sum F_x = 0 \rightarrow P &= F_R \cos \alpha_R - F_L \cos \alpha_L = \frac{AE}{L_{OB}} \Delta_{AE} \cos \alpha_R - \frac{AE}{L_{OD}} \Delta_{DH} \cos \alpha_L \\ &= \frac{AE}{0.5L_t} \Delta_{AE} \cos \alpha_R - \frac{AE}{0.5L_t} \Delta_{DH} \cos \alpha_L = \frac{2AE}{L_t} (\Delta_{AE} \cos \alpha_R - \Delta_{DH} \cos \alpha_L) \rightarrow \\ P &= \frac{2AE}{L_t} \left[\begin{aligned} & \Delta_{AE} \times \frac{(l_b + \delta) - u \cos \theta + v \sin \theta}{\sqrt{((l_b + \delta) - u \cos \theta + v \sin \theta)^2 + (h_c - u \sin \theta - v \cos \theta)^2}} \\ & + \Delta_{DH} \times \frac{(-l_b + \delta) + u \cos \theta + v \sin \theta}{\sqrt{((-l_b + \delta) + u \cos \theta + v \sin \theta)^2 + (h_c + u \sin \theta - v \cos \theta)^2}} \end{aligned} \right] \end{aligned} \quad (18)$$

where F_R and F_L are the forces of the right and the left cables, respectively. l_t is the total length of cables.

Equations (19) and (20) can be used for plotting the strain curves of cables versus lateral displacement of the frame.

$$\varepsilon_R = \frac{\Delta_{AE}}{L_{AE} + L_{EO}} \quad (19)$$

$$\varepsilon_L = \frac{\Delta_{DH}}{L_{DH} + L_{HO}} \quad (20)$$

The obtained equations are valid until one of the cables is totally straightened. At that moment, the

$$\begin{aligned} \Delta_{DH} &= \\ \frac{1}{2} \sqrt{((l_b - \delta) - u \cos \theta - v \sin \theta)^2 + (-h_c - u \sin \theta + v \cos \theta)^2} & \\ - \frac{1}{2} \sqrt{(l_b - u)^2 + (h_c - v)^2} & \end{aligned} \quad (14)$$

The main equation below is obtained by putting the above equations in the equilibrium equation of cylinder (equation (4)). This is an implicit relation and makes the cylinder rotation and frame lateral displacement dependent on each other.

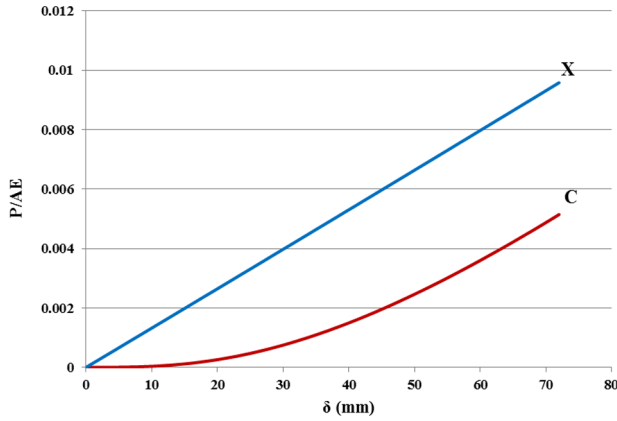


Figure 5. $P - \delta$ curves for hinged frame with cross-cable and cylinder-cable bracings.

force of the other cable becomes 0, since $\sum M = 0$ should be satisfied. After that, the next cable starts to loosen and the slopes of the internal and external cables are equal for the active cable.

The frame lateral displacement when one of the cables is straightened is called δ_{sr} .

For frame lateral displacement greater than δ_{sr} , one wire does not work anymore. In this case if frame lateral displacement is δ and the angle between diagonal direction of AC and horizontal direction is θ , elongation of AC is $\delta \cos \theta$. Regarding this subject, the strain of another cable and lateral force of the story are expressed in terms of the lateral displacement of the frame in the cross-cable bracing system as follows:

$$\delta_{AC} = \delta \cos \theta = \delta \frac{l_b}{\sqrt{l_b^2 + h_c^2}}, \tag{21}$$

$$l_{AC} = \sqrt{l_b^2 + h_c^2} \rightarrow \varepsilon = \varepsilon_{AC} = \frac{\delta_{AC}}{l_{AC}} = \delta \frac{l_b}{l_b^2 + h_c^2}$$

$$\begin{aligned} \sum F_X = 0 \rightarrow P = F_{AC} \cos \theta = A\sigma_{AC} \cos \theta = AE\varepsilon_{AC} \cos \theta \rightarrow \\ P = AE \frac{l_b}{l_b^2 + h_c^2} \delta \times \frac{l_b}{\sqrt{l_b^2 + h_c^2}} = \frac{l_b^2}{(l_b^2 + h_c^2)^{\frac{3}{2}}} AE\delta \end{aligned} \tag{22}$$

Figure 5 shows the curve of force–displacement for the hinged frame with cross-cable bracing and cylinder-cable bracing. The beam length is 4 m, the height of the column is 3 m, the length of the horizontal cylinder is 22 cm, and the internal diameter of the cylinder minus cable diameter is 5 cm.

In Figure 5, X and C curves correspond to cross-cable bracing and cylinder-cable bracing, respectively.

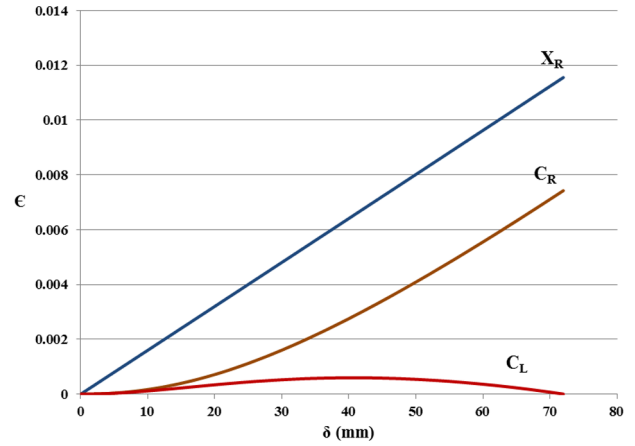


Figure 6. $\varepsilon - \delta$ curves of cables in the cross-cable and cylinder-cable bracings.

According to the figure, the stiffness of cylinder-cable bracing system is not constant. The initial stiffness is 0 which increases with an increase in the frame lateral displacement.

Figure 6 shows the strain curves of cables versus lateral displacement for the hinged frame with the mentioned dimensions. Equations (19) and (20) have been used in plotting the curves.

In this figure, X corresponds to the right cable of the cross-cable bracing and C_R and C_L to the right and left cables of the cylinder-cable bracing, respectively.

Using cables as the cross bracing in building frames is confronted with basic difficulties. Figure 6 shows two main advantages of cylinder-cable bracing over cross-cable bracing. According to this figure, first, the cable will reach its final strength at a higher displacement in the cylinder-cable bracing. Consequently, the frame ductility increases; hence, the ductility defect of the cable is solved. Second, both cables are under tension in a considerable load range and none of them will be loosened under frame lateral displacement. Therefore, the impulses caused by cable loosening are removed.

If the displacement is toward the right, the force will be 0 in the left cable at the displacement δ_{sr} where the right cable is straightened.

The cylinder dimensions should be selected in such a way that, first, δ_{sr} is equal to or slightly higher than the displacement of the frame’s damage limit in order to ensure that both cables are under tension. Second, the cable reaches its final strength at the frame’s damage limit displacement for optimal use of cable strength and frame ductility.

Prestressing effects of cables

If the prestressing force is F_p in the cables, the cylinder rotation and lateral displacement of the frame can be depended on each other, giving rise to the $\sum M = 0$ equation. In such cases, concerning the equality of axial rigidity and cables lengths, the moment equilibrium of the cylinder is expressed as follows:

$$P = \frac{2AE}{l_t} \left[\begin{aligned} & \left(\Delta_{AE} + \frac{F_p l_t}{2AE} \right) \times \frac{(l_b + \delta) - u \cos \theta + v \sin \theta}{\sqrt{((l_b + \delta) - u \cos \theta + v \sin \theta)^2 + (h_c - u \sin \theta - v \cos \theta)^2}} \\ & + \left(\Delta_{DH} + \frac{F_p l_t}{2AE} \right) \times \frac{(-l_b + \delta) + u \cos \theta + v \sin \theta}{\sqrt{((-l_b + \delta) + u \cos \theta + v \sin \theta)^2 + (h_c + u \sin \theta - v \cos \theta)^2}} \end{aligned} \right] \quad (28)$$

$$\begin{aligned} & \left(\frac{l_t}{2AE} F_p + \Delta_{AE} \right) \times \left| \frac{\vec{AE} \times \vec{EG}}{\vec{AE}} \right| \\ & = \left(\frac{l_t}{2AE} F_p + \Delta_{DH} \right) \times \left| \frac{\vec{DH} \times \vec{FH}}{\vec{DH}} \right| \end{aligned} \quad (23)$$

Putting equations (5) to (14) in equation (23), an implicit equation is obtained in equation (24), regarding the prestressing effects. This equation makes the cylinder rotation and lateral displacement of the frame dependent on each other.

$$\begin{aligned} & \rightarrow \left[\frac{l_t}{AE} F_p + \sqrt{((l_b + \delta) - u \cos \theta + v \sin \theta)^2 + (h_c - u \sin \theta - v \cos \theta)^2} - 2l_e \right] \\ & \times \frac{|(l_b + \delta)(u \sin \theta + v \cos \theta) - h_c(u \cos \theta - v \sin \theta)|}{\sqrt{((l_b + \delta) - u \cos \theta + v \sin \theta)^2 + (h_c - u \sin \theta - v \cos \theta)^2}} \\ & = \left[\frac{l_t}{AE} F_p + \sqrt{((-l_b + \delta) + u \cos \theta + v \sin \theta)^2 + (h_c + u \sin \theta - v \cos \theta)^2} - 2l_e \right] \\ & \times \frac{|(-l_b + \delta)(-u \sin \theta + v \cos \theta) + h_c(u \cos \theta + v \sin \theta)|}{\sqrt{((-l_b + \delta) + u \cos \theta + v \sin \theta)^2 + (h_c + u \sin \theta - v \cos \theta)^2}} \end{aligned} \quad (24)$$

where l_t is the total length of each cable and l_e is the length of the external parts of the cables. If l_i is the cable length in the cylinder, then $l_t = 2l_e + l_i$.

The resultant horizontal force of the cables is as follows:

$$P = F_R \cos \alpha_R - F_L \cos \alpha_L \quad (25)$$

The forces of the cables are defined as follows:

$$F_R = \frac{AE}{l_t} \Delta_R + F_p \xrightarrow{\Delta_R = 2\Delta_{AE}} F_R = \frac{2AE}{l_t} \left(\Delta_{AE} + \frac{F_p l_t}{2AE} \right) \quad (26)$$

$$F_L = \frac{AE}{l_t} \Delta_L + F_p \xrightarrow{\Delta_L = 2\Delta_{DH}} F_L = \frac{2AE}{l_t} \left(\Delta_{DH} + \frac{F_p l_t}{2AE} \right) \quad (27)$$

where Δ_R and Δ_L are the elongation of the right and left cables, respectively.

Equation (28) is obtained by putting the last two equations into equation (25).

Equation (28) is used for plotting P - δ curve.

The strain curves of the cables are plotted versus lateral displacement of the frame using the formulas below

$$\varepsilon_R = \frac{2\Delta_{AE}}{l_t} + \frac{F_p}{AE} \quad (29)$$

$$\varepsilon_L = \frac{2\Delta_{DH}}{l_t} + \frac{F_p}{AE} \quad (30)$$

Figure 7 shows the curve of the lateral force versus the lateral displacement of the hinged frame with cylinder-cable bracing for the prestressing forces corre-

sponding to 0, 200, 400, 600, and 800 N/mm². The beam length is taken as 4 m, column height as 3 m, cylinder length as 22 cm, and the internal diameter of the cylinder minus the cable diameter as 5 cm. The cylinder is placed horizontally.

According to Figure 7, the initial stiffness of the cylinder-cable bracing system is proportional to the prestressing force. If there is no prestressing force in the cables, then the initial stiffness of the frame with cylinder-cable bracing will be equal to that of the frame without bracing. The considered stiffness will be achieved by applying a certain prestressing force.

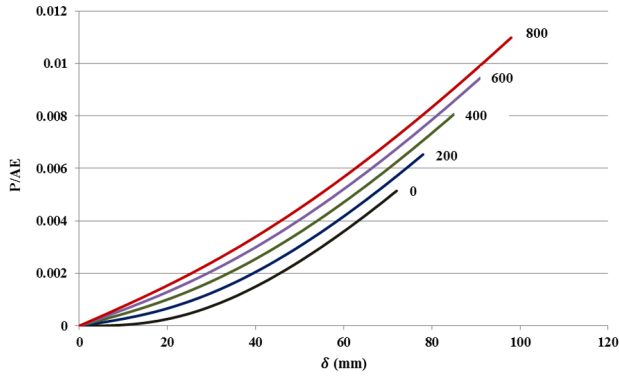


Figure 7. The effect of prestressing on the $P - \delta$ curve of cylinder-cable bracing.

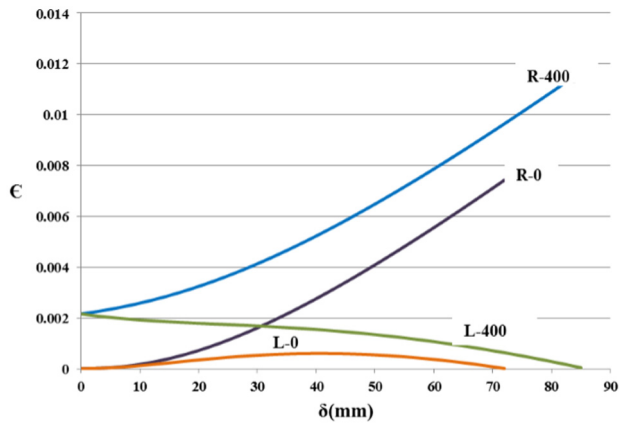


Figure 8. Prestressing effect of cables on their $\epsilon - \delta$ curves in cylinder-cable bracing.

Figure 8 shows the curves of the cable strain versus the lateral displacement of the frame for cylinder-cable bracing in two statuses: without prestressing force and with prestressing stress of 400 N/mm^2 . Lateral displacement of the frame is assumed to be toward the right in plotting the curves. The label of each curve indicates the value of the prestressing stress. Letters *R* and *L* correspond to the prestressing stress of the right and left cables, respectively.

According to Figure 8, in case of increasing prestressing stress, the values of δ_{sr} increase and the cables reach strain yielding at smaller displacements.

The effect of rigid cylinder dimensions on the behavior of cylinder-cable bracing

Cylinder dimensions are the effective parameters in the behavior of cylinder-cable bracing. These dimensions should be selected in such a way to make the cable crooked. In order to show the effect of the cylinder

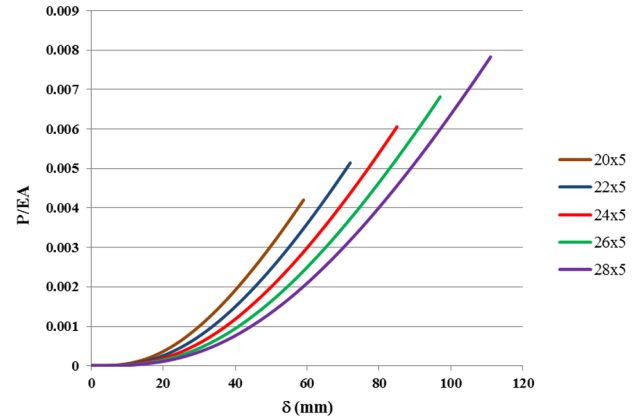


Figure 9. The effect of cylinder length on $P - \delta$ curves.

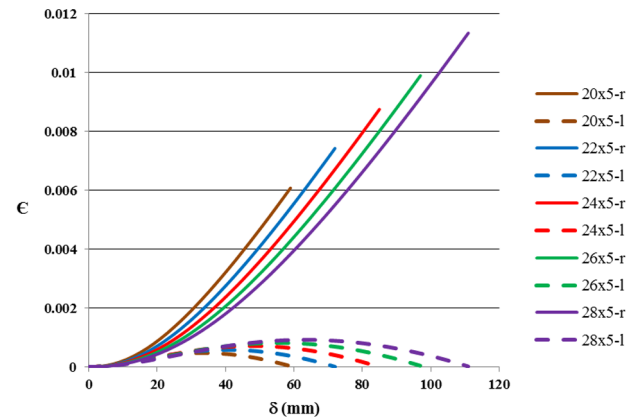


Figure 10. The effect of cylinder length on $\epsilon - \delta$ curve.

when it is in a horizontal position, an equation is defined below:

$$\frac{u}{v} > \frac{l_b}{h_c} \quad (31)$$

In other words, if the cylinder is placed horizontally, the slope inside the cylinder should be lower than the one outside. The more the difference between these slopes, the more the difference between the behaviors of the cylinder-cable and the cross-cable bracings. If the dimensions of the cylinder are such that the slopes of the cables are equal inside and outside the cylinder, then the behaviors of the cylinder-cable and cross-cable bracing are exactly the same.

The effect of cylinder length

In order to study the effect of cylinder length, $P - \delta$ curve of bracing and $\epsilon - \delta$ curves of the cables have been plotted in Figures 9 and 10, respectively. These figures

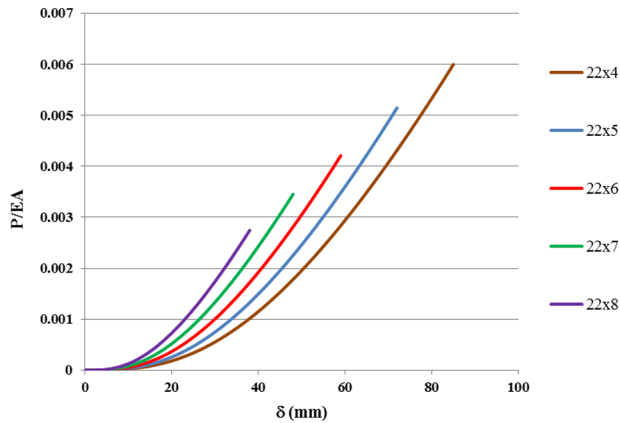


Figure 11. The effect of internal diameter of the cylinder on $P - \delta$ curve.

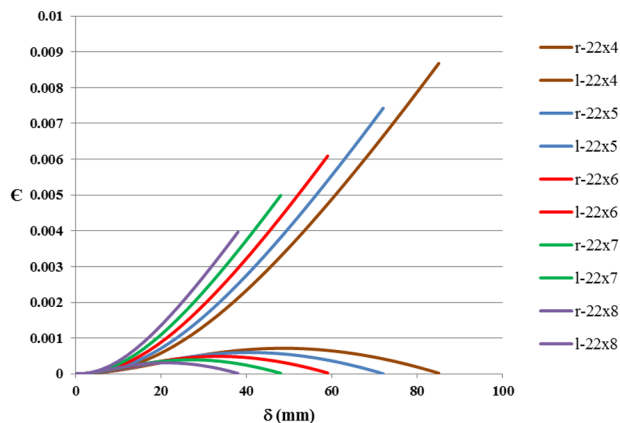


Figure 12. The effect of internal diameter of the cylinder on $\epsilon - \delta$ curve.

are plotted for the hinged frame with beam length of 4 m, column height of 3 m, and cylinder-cable bracing; the internal diameter of the cylinder minus the cable diameter is 5 cm and the cylinder lengths are 20, 22, 24, 26, and 28 cm.

Concerning the $P-\delta$ curves of the cylinders with different lengths, it is observed that the increase in cylinder length results in an increase in δ_{sr} . Moreover, the curves of the cylinders with longer lengths are below the curves of those with smaller lengths.

As observed in Figure 10, the increase in cylinder length causes the cables to reach yielding limit at larger displacement.

The effect of internal diameter of cylinder

The $P-\delta$ and $\epsilon-\delta$ curves have been plotted for the frame with the mentioned dimensions and presented in Figures 11 and 12, respectively. The length of the

cylinder is constant and equal to 22 cm, and the internal diameter of the cylinder minus the cable diameter is 4, 5, 6, 7, and 8 cm.

Concerning the curves plotted for the cylinders with different internal diameters, the decrease in the internal diameter of the cylinder will end in an increase in δ_{sr} . Besides, the curves which correspond to the cylinders with smaller diameters are located below those of the cylinders with larger diameters.

According to Figure 12, the decrease in the internal diameter of the cylinder will cause the cables to reach the yielding limit at a larger displacement.

The series of curves related to the internal diameter of the cylinder shows how ignoring the cable diameter might cause errors in the calculations. For plotting the steel cylinder wire-ropes more accurately and closer to the reality, the dimensions of cylinder or the parameters u and v should be considered as variables (the cylinder has been assumed rigid initially; $U = U_0$ and $V = V_0$). This consideration is because of the loads applied to the cylinder at the cylinder to wire-rope contact area, due to the wire-ropes not being straight, causing the reduction in the diameter and the length of the cylinder. For example, if the internal diameter of the cylinder is 5 cm and wire-rope diameter is 1 cm, then $U = 4$ cm (the “22 × 4” curves in Figures 11 and 12). The curves of these figures have been plotted with rigidity assumption of cylinder. Now, if the 22 × 4 are plotted considering the deformations of cylinder, then the contact forces between wire-ropes and cylinder are 0 for lateral displacements of $\delta = 0$ and $\delta = \delta_s$, therefore $U = U_0$ and $V = V_0$. Consequently, these curves are coincident with the 22 × 4 of Figures 11 and 12 for the mentioned lateral displacements. For intermediate statuses ($0 < \delta < \delta_s$), as the diameter of cylinder increases very slightly, the 22 × 4 curves of previous state (considering the deformations of cylinder) also approach to the “22 × 5” curves very slightly ($u = 5$).

Numerical validation

To validate the constitutive formulas, presented in this research, the tri-dimensional model of the considered frame was modeled in the well-known commercial finite element (FE) software package ABAQUS. For this purpose, the portal frame with cable-cylinder bracing has been modeled tri-dimensionally. The beam length was 4 m, column height 3 m, cylinder length 22 cm, internal diameter of cylinder minus cable diameter 5 cm, the sections of beam and column from box section $100 \times 100 \times 8$ mm, and the cross-sectional area of cable 1 cm^2 . The cylinder is considered as rigid. The FE model is shown in Figure 13.

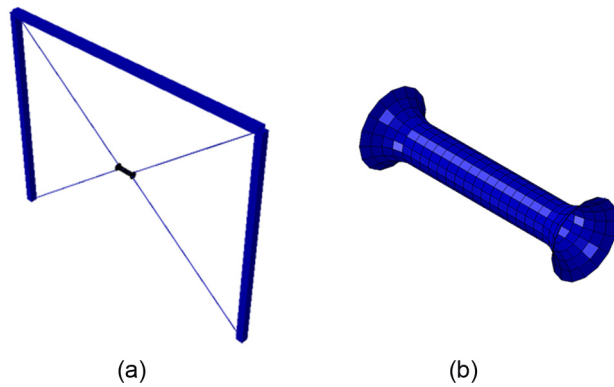


Figure 13. FE-adopted 3D model: (a) cable-cylinder braced frame and (b) cylinder mesh.

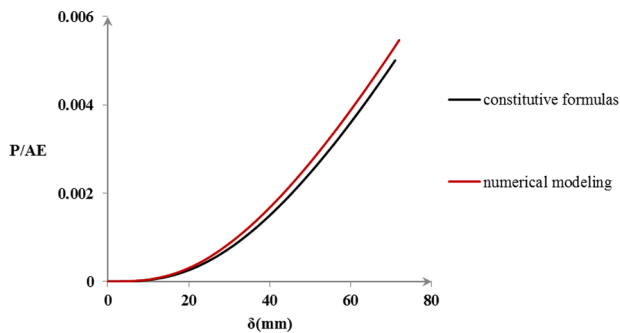


Figure 14. Comparison of $P - \delta$ curves of constitutive formulas with numerical modeling.

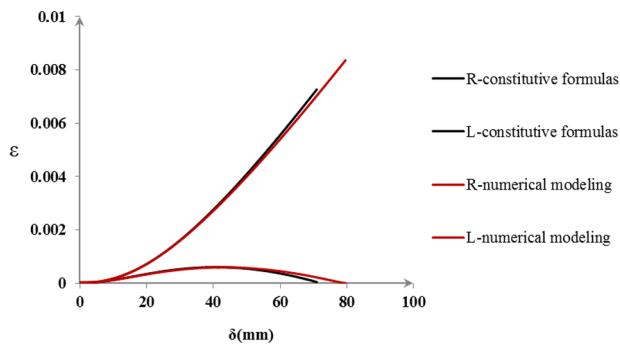


Figure 15. Comparison of $\varepsilon - \delta$ curves of constitutive formulas with numerical modeling.

$P - \delta$ and $\varepsilon - \delta$ curves, obtained from the resulted constitutive formulas and numerical modeling have been compared with each other in Figures 14 and 15, respectively. The letters *R* and *L* in Figure 13 correspond to the right and left cables, respectively, which are connected to the right and left columns, respectively. Based on the mentioned figures, the results obtained from constitutive formulas are in relatively good

agreement with those of numerical modeling. Slight differences between the curves can be referred to the axial deformation of columns and beam. This deformation has been ignored in the curves obtained from theoretical relations. Moreover, the contact between the cylinder and cables has been modeled more realistically in the tri-dimensional model and the cable can slide on the cylinder under lateral displacement of the frame, while in the two-dimensional model, the cables, inside and outside of the cylinder, have been considered as separate elements adjoined to each other by a hinge.

Conclusion

This research presents the equations governing the behavior of stiff cylinder-cable bracing (like steel cylinder). Based on the studies conducted here, the behavior of cylinder-cable bracing is a function of cable stiffness (AE), cylinder dimensions, and also prestressing forces of the cables. The stiffness of the cylinder-cable bracing is not constant and increases in accordance with frame lateral displacement. The considered stiffness can be achieved at smaller displacements with increasing prestressing forces of cables.

In order to show their effects, the dimensions of the cylinder in the cylinder-cable bracing should be selected in such a way to create a crook along the cable.

The more the difference between the cable angles inside and outside the cylinder, the more the difference between the behaviors of cylinder-cable and cross-cable bracings.

The cables reach the yielding limit at larger frame lateral displacements with increasing cylinder length. The $P - \delta$ curves (e.g. Figures 5 and 7) of the bracings with longer cylinder are observed below those of the bracings with shorter cylinder.

The effect of decreasing the internal diameter of the cylinder is similar to that of increasing the cylinder length. Cylinder-cable bracing has two advantages over cross-cable bracing:

1. The cables reach their final strengths at larger displacements, and consequently the frame ductility increases; therefore, the ductility defect of cables is solved.
2. Both cables are under tension in a considerable range of loading and none of them will loosen under frame lateral displacement. Therefore, the impulse caused by cable loosening is removed.

The dimensions of the cylinder and the prestressing of cables should be determined in such a way that the

cables reach their final strengths in the damage displacement limit of the frame in order to use optimally the cable strength and frame ductility.

Declaration of Conflicting Interests

The author(s) declared no potential conflicts of interest with respect to the research, authorship, and/or publication of this article.

Funding

The author(s) received no financial support for the research, authorship, and/or publication of this article.

References

- Ben Mekki O and Auricchio F (2011) Performance evaluation of shape-memory-alloy superelastic behavior to control a stay cable in cable-stayed bridges. *International Journal of Non-Linear Mechanics* 46(2): 470–477. DOI: 10.1016/j.ijnonlinmec.2010.12.002.
- Cai J, Xu Y, Zhuang L, et al. (2012) Comparison of various procedures for progressive collapse analysis of cable-stayed bridges. *Journal of Zhejiang University: Science A* 13(5): 323–334. DOI: 10.1631/jzus.A1100296.
- Chuang S, Zhuge Y and McBean PC (2004) Seismic retrofitting of unreinforced masonry walls by cable system. In: *Proceedings of the 13th world conference on earthquake engineering*, Vancouver, BC, Canada, 1–6 August.
- Fanaie N, Aghajani S and Shamloo S (2012) Theoretical assessment of wire rope bracing system with soft central cylinder. In: *Proceedings of the 15th world conference on earthquake engineering*, Lisbon, 24–28 September.
- Hadi M and Saeed Alrudaini T (2012) New building scheme to resist progressive collapse. *Journal of Architectural Engineering* 18(4): 324–331. DOI: 10.1061/(ASCE)AE.1943-5568.0000088.
- Hou X and Tagawa H (2009) Displacement-restraint bracing for seismic retrofit of steel moment frames. *Journal of Constructional Steel Research* 65(5): 1069–1104. DOI: 10.1016/j.jcsr.2008.11.008.
- Jeong-In S and Sung Pil C (2000) Experimental study on fatigue behaviour of wire ropes. *International Journal of Fatigue* 22(4): 339–347. DOI: 10.1016/S0142-1123(00)00003-7.
- Kang H, Zhao Y and Zhu H (2014) Analytical and experimental dynamic behavior of a new type of cable-arch bridge. *Journal of Constructional Steel Research* 101: 385–394. DOI: 10.1016/j.jcsr.2014.06.005.
- Keun-Hyeok Y, Gwang-Hee K and Hong-Suk Y (2011) Shear behavior of continuous reinforced concrete T-beams using wire rope as internal shear reinforcement. *Construction and Building Materials* 25(2): 911–918. DOI: 10.1016/j.conbuildmat.2010.06.093.
- Kurata M, Leon R and DesRoches R (2012) Rapid seismic rehabilitation strategy: concept and testing of cable bracing with couples resisting damper. *Journal of Structural Engineering: ASCE* 138(3): 354–262. DOI: 10.1061/(ASCE)ST.1943-541X.0000401.
- Osamu H, Kouhei S and Taro M (1999) The role of cables in large span spatial structures: introduction of recent space structures with cables in Japan. *Engineering Structures* 21(8): 795–804. DOI: 10.1016/S0141-0296(98)00032-7.
- Razavi M and Sheidaii MR (2012) Seismic performance of cable zipper-braced frames. *Journal of Constructional Steel Research* 74: 49–57. DOI: 10.1016/j.jcsr.2012.02.007.
- Saleem MA and Saleem MM (2010) Cable bracing system to resist wind forces on tall building in Miami. In: *Proceedings of the 3rd fib international congress*, Washington, DC, 29 May–2 June.
- Straupe V and Paeglitis A (2013) Analysis of geometrical and mechanical properties of cable-stayed bridge (Modern building materials, structures and techniques). *Procedia Engineering* 57: 1086–1093. DOI: 10.1016/j.proeng.2013.04.137.
- Tan S and Astaneh-Asl A (2003) Use of steel cables to prevent progressive collapse of existing buildings. In: *Proceedings of sixth conference on tall buildings in seismic regions*, Los Angeles, CA, 4 June.
- Wu H, Xiang Y and Wang J (2006) Condition assessment of long span cable-stayed bridge. *Journal of Zhejiang University: Science A* 7(2): 297–308. DOI: 10.1631/jzus.2006.AS0297.
- Zahrai SM and Hamidia MJ (2009) Studying the rehabilitation of existing structures using compound system of cables and shape memory alloys. In: *Proceedings of the ATC and SEI conference on improving the seismic performance of existing buildings and other structures*, San Francisco, CA, 9–11 December.